



# GRK5 deficiency decreases diet-induced obesity and adipogenesis

Feifei Wang<sup>1</sup>, Li Wang<sup>1</sup>, Minjie Shen, Lan Ma<sup>\*</sup>

The State Key Laboratory of Medical Neurobiology and Pharmacology Research Center, Shanghai Medical College and Institutes of Brain Science, Fudan University, Shanghai 200032, China

## ARTICLE INFO

### Article history:

Received 3 March 2012

Available online 7 April 2012

### Keywords:

White adipose tissue

High-fat diet

Preadipocyte

Lipogenesis

## ABSTRACT

Identification of the protein factors that regulate the adipogenesis and lipid metabolism of adipose tissue is critical for the understanding of the physiology and pathology of obesity and energy homeostasis. In this study, we found that G protein coupled receptor (GPCR) kinase 5 (GRK5) was expressed at a relatively high level in the white adipose tissue. When fed on a high-fat diet, GRK5<sup>-/-</sup> mice gained significantly less weight and had decreased WAT mass than their wild type littermates, which could not be attributed to alterations in food consumption or energy expenditure. However, GRK5<sup>-/-</sup> mice showed a 30–70% decreased expression of lipid metabolism and adipogenic genes in WAT. Moreover, GRK5<sup>-/-</sup> embryonic fibroblasts and preadipocytes exhibited 40–70% decreased expression of adipogenic genes and impaired adipocyte differentiation when induced in vitro. Taken together, these results suggest that GRK5 is an important regulator of adipogenesis and is crucial for the development of diet-induced obesity.

© 2012 Elsevier Inc. All rights reserved.

## 1. Introduction

Obesity, characterized by increased mass of adipose tissues, presents a risk to health and may lead to the development of metabolic syndrome, diabetes, and cardiovascular disease under pathophysiological conditions [1,2]. The increased mass of adipose tissues was largely attributed to adipocyte hypertrophy (cell size increase) and hyperplasia (cell number increase) and could store excess energy intake. Hyperplastic growth appears only at early stages in adipose tissue development [3], while hypertrophy occurs prior to meet the need for additional fat storage capacity in the progression of obesity [4]. Elucidating the regulation of adipogenesis and lipogenesis of adipose tissue is thus of critical importance for the understanding the processes that lead to obesity and related pathological conditions.

G protein-coupled receptor (GPCR) kinases (GRKs) specifically phosphorylate serine/threonine residues located on the cytoplasmic loops and C terminus of the receptors. Phosphorylation of a GPCR by GRK promotes the high affinity binding of arrestins and

**Abbreviations:** ANOVA, analysis of variance; GPCR, G protein-coupled receptor; GRK, GPCR kinase; KO, knockout; SD, standard diet; HFD, high fat diet; WAT, white adipose tissue; MEF, mouse embryonic fibroblast; SVF, stromal vascular fraction cell; PPAR $\gamma$ , peroxisome proliferator-activated receptor- $\gamma$ ; C/EBP, CCAAT/enhancer binding protein; PBS, phosphate buffered saline; EDTA, ethylene diamine tetraacetic acid; IBMX, isobutylmethylxanthine; DMX, dexamethasone.

<sup>\*</sup> Corresponding author. Fax: +86 21 54237621.

E-mail address: [lanma@shmu.edu.cn](mailto:lanma@shmu.edu.cn) (L. Ma).

<sup>1</sup> These authors contributed equally to this work.

induces receptor internalization, and thus feed-back inhibits GPCR responses to extracellular signals [5,6]. The in vivo physiological functions of various subtypes of GRKs (GRK1–7) have been previously ascribed to phosphorylating and desensitizing specific GPCRs [7,8]. However, recent evidence also indicates that GRKs may also possess non-catalytic function and target to non-GPCR substrates in vivo. For example, GRK2 can interact with Gq/11 and function independently of its kinase activity to inhibit insulin-mediated glucose transport stimulation, and can also form a complex with IRS1 and regulate insulin signaling in skeletal muscle and adipose tissues [9,10]. Our recent studies indicate that GRK2 interact with PTCH1 in a kinase activity independent manner and regulates cyclin B1 and zebrafish embryonic development [11]. The localization of GRK5 in the nucleus and its role in regulation of gene expression has been reported. GRK5 is a nuclear HDAC kinase that plays a key role in G $\alpha$ q-dependent transcriptional regulation and maladaptive cardiac hypertrophy [12]. GRK5 was also shown to interact with I $\kappa$ B $\alpha$ , and inhibits NF $\kappa$ B-mediated transcriptional responses [13]. GRK5 can phosphorylate p53 and regulate p53-mediated gene expression and apoptosis in response to DNA damage [14]. These results implicate that GRK5 may play an important role in gene transcription to regulate many aspects of physiology.

In current study, we found that GRK5 was upregulated in WAT of high fat diet (HFD)-feeding mice. Under HFD, decreased fatty acid metabolism and adipogenic gene transcription, adipogenesis and diet-induced obesity were observed in GRK5 deficient mice. Our results suggest that GRK5 plays a key role in regulation of WAT function in physiological and pathological conditions such as diet-induced obesity.

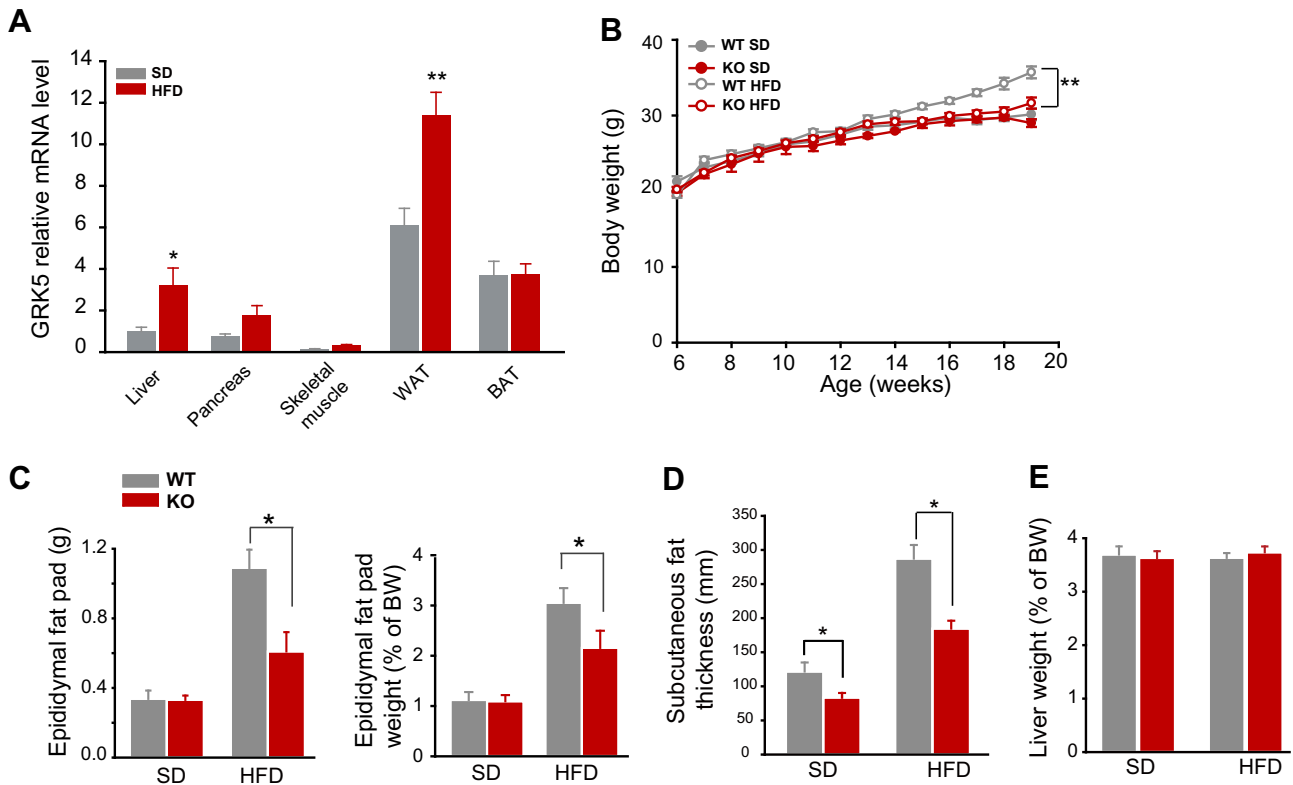


**Fig. 1.** GRK5<sup>-/-</sup> mice were resistant to HFD-induced obesity. (A) Quantitative RT-PCR analysis for relative GRK5 mRNA level in various tissues from mice fed on SD or HFD. \**P* < 0.05, \*\**P* < 0.01 vs. SD group. (B) Body weights of WT and GRK5<sup>-/-</sup> mice fed on a SD (*n* = 10) or HFD (*n* = 15) since week 6. (C–E) 20-week-old WT and GRK5<sup>-/-</sup> mice fed on SD or HFD for 14 weeks. Epididymal fat pad weight (C), subcutaneous fat thickness (D), and liver weight (E) in SD- and HFD-fed WT and GRK5<sup>-/-</sup> mice are plotted. *n* = 6–8 for each group, \**P* < 0.05 vs. WT group.

## 2. Materials and methods

### 2.1. Mouse maintenance

GRK5<sup>+/-</sup> C57BL/6 mice were provided by R.J. Lefkowitz and R.T. Premont (Duke University Medical Center, Durham, NC, USA). GRK5 deficient (GRK5<sup>-/-</sup>) C57BL/6 mice and their wild-type (WT) littermates were obtained from self-crossing of GRK5 heterozygous mice. Genotyping was carried out by PCR amplification using tail tip DNA as described [15]. Mice were housed in groups and maintained on a 12 h light/dark cycle with food and water available *ad libitum*. Mice were fed a standard diet (SD, 10% fat, 70% carbohydrates, and 20% proteins) or HFD (45% fat, 35% carbohydrates, and 20% proteins), starting at 6 weeks of age for 13–16 weeks. Body weight was monitored on a weekly basis for mice. All animal treatments were strictly in accordance with the National Institutes of Health Guide for the Care and Use of Laboratory Animals.

### 2.2. Measurement of food intake and metabolism

20-week-old WT and GRK5<sup>-/-</sup> mice (*n* = 6–8 per genotype) were placed in a metabolic cage connected to an open-circuit, indirect calorimetric system, with the air flow adjusted to 0.5 L/min. The temperature in the metabolic cage (24 ± 1 °C) was stable and controlled throughout the experiment. Average daily food intake, Oxygen consumption (*V*<sub>O2</sub>), and Carbon dioxide production (*V*<sub>CO2</sub>) were recorded at 10-s intervals, measured for 24 h using the Comprehensive Laboratory Monitoring System (CLAMS; Columbus Instruments, Columbus, Ohio, USA). Respiratory quotient (RQ) was calculated as a ratio of *V*<sub>CO2</sub> to *V*<sub>O2</sub>.

### 2.3. RNA extraction and real-time PCR analysis

Mouse tissues were isolated, rinsed in PBS, frozen in liquid nitrogen and stored at -70 °C until extraction. Total RNA was extracted from tissues using the RNeasy Lipid Tissue Kit (Qiagen GmbH, Hilden, German) according to the manufacturer's instructions with the inclusion of a DNase digestion step. The Superscript First-Strand Synthesis System for RT-PCR (Invitrogen Life Technologies, Gaithersburg, MD, USA) was used with random primers for reverse transcription. Quantitative RT-PCR amplification of the cDNA was performed on samples in triplicate with Power SYBR Green PCR Master Mix (TAKARA, Shiga, Japan) using the Applied Biosystems 7900HT Fast Realtime PCR System (Applied Biosystems, Foster City, CA, USA). Target gene mRNA expression was normalized to the internal control GAPDH.

### 2.4. Immunohistochemistry and Oil Red O staining

Tissues fixed in 4% paraformaldehyde were processed and subjected to dehydration in increased sucrose (20–30% sucrose). Sections (20 μm) prepared from tissue frozen in O.C.T. compound were mounted on coverslips for staining with hematoxylin–eosin (Vector Laboratories, Burlingame, CA, USA), and the differentiated cells were stained with Oil Red O dye (saturated Oil Red O dye in six parts of isopropanol and four parts of water), an indicator of cell lipid content, and then exhaustively rinsed with water. The sections were washed, and the coverslips were mounted on slides, and examined by confocal fluorescence microscopy (Zeiss 510; Carl Zeiss, Jena, Germany).

## 2.5. Adipogenesis

Mouse embryonic fibroblasts (MEFs) prepared from 13.5 day embryos were digested in 10 ml 0.05% trypsin/PBS at 37 °C for 30 min. Cells were collected by centrifugation at 650g for 10 min, plated onto 10 cm culture dishes at  $1.5 \times 10^6$  cells/dish, and cultured in 10 ml of Dulbecco's modified Eagle's medium (DMEM) with 10% fetal bovine serum (Invitrogen) until confluence. MEFs were split, and adipogenesis was induced in DMEM containing 0.5 mM IBMX (Sigma), 1  $\mu$ M DMX (Sigma), 1  $\mu$ M insulin (Sigma), and 0.5 mM rosiglitazone (Sigma) for 6 days. Cells were then maintained in medium containing 1  $\mu$ M insulin and 0.5 mM rosiglitazone for 3 days. The medium was replenished at 2 day intervals. For adipogenesis of primary white preadipocytes, stromal vascular fraction cells (SVFs) from adult tissue were isolated from epididymal fat pads of 6–8 week-old mice. Cells were plated at a density of  $1-3 \times 10^6$ /10 cm dish until confluence before induction of adipogenesis. Cells were incubated in DMEM/F12 supplemented with 0.5 mM IBMX, 1  $\mu$ M DMX, and 1  $\mu$ M insulin for 3 days, and then changed to medium containing only 1  $\mu$ M insulin for another 3 days. The medium was replenished at 2 day intervals.

## 2.6. Statistical analysis

The results were assessed by two-tail Student's *t*-test to compare two groups or by one-way ANOVA with Tukey post hoc test for multiple comparisons using Sigma Stat (Systat Software, San Jose, CA, USA). For assessment of weight gain, data were analyzed by two-way ANOVA with repeated measurements. Statistical comparison between 2 genotypes within the same treatment group and between different treatment groups within the same genotype were carried out for each experiment. In all tables and figures, data are expressed as means  $\pm$  standard error (SE), and all significant differences are given in the figures or figure legends.

## 3. Results

### 3.1. GRK5 was abundantly expressed in adipose tissues and GRK5 ablation prevented HFD-induced obesity

As shown by quantitative PCR analysis, GRK5 was expressed at relatively high levels in white adipose tissue (WAT) and brown adipose tissue (BAT) depots in wild type (WT) C57BL/6 mice on standard diet (SD), while it was barely detectable in skeletal muscle and at very low levels in liver and pancreas (Fig. 1A). Additionally, the GRK5 mRNA level in WAT and liver rose markedly in mice fed with a HFD (Fig. 1A).

GRK5<sup>-/-</sup> (KO) mice were assessed to explore the potential role of GRK5 in adipocyte physiology. Although when fed on a SD, the total body weights of GRK5<sup>-/-</sup> mice were not different from their WT littermates, GRK5<sup>-/-</sup> mice gained weight at a slower rate than WT littermates when challenged with a HFD (Fig. 1B). By 19 weeks old, WT mice fed a HFD had a significantly higher average body weight than those fed on SD ( $35.7 \pm 0.7$  vs.  $30.2 \pm 0.8$ ,  $P < 0.01$ ), whereas the body weights for GRK5<sup>-/-</sup> mice fed on HFD were not different from GRK5<sup>-/-</sup> ( $31.0 \pm 0.6$  vs.  $29.0 \pm 0.5$ ,  $P > 0.10$ ) or WT littermates fed on SD ( $31.0 \pm 0.6$  vs.  $30.2 \pm 0.8$ ,  $P > 0.48$ ) (Fig. 1B).

The organs from WT and GRK5<sup>-/-</sup> mice fed on HFD were examined next. Most organs showed no obvious difference in size between the two genotypes. The lower body weight of GRK5<sup>-/-</sup> mice fed on HFD could be largely accounted for by a reduction in epididymal WAT weight (Fig. 1C). Moreover, ablation of GRK5 also resulted in a significant reduction of subcutaneous fat thickness (Fig. 1D). No significant difference in weight of BAT (data not shown) or liver was observed (Fig. 1E).

### 3.2. GRK5 deficiency did not increase energy expenditure and lipolysis

Resistance to the increase of body weight may result from an imbalance of food intake and energy expenditure. Thus, food

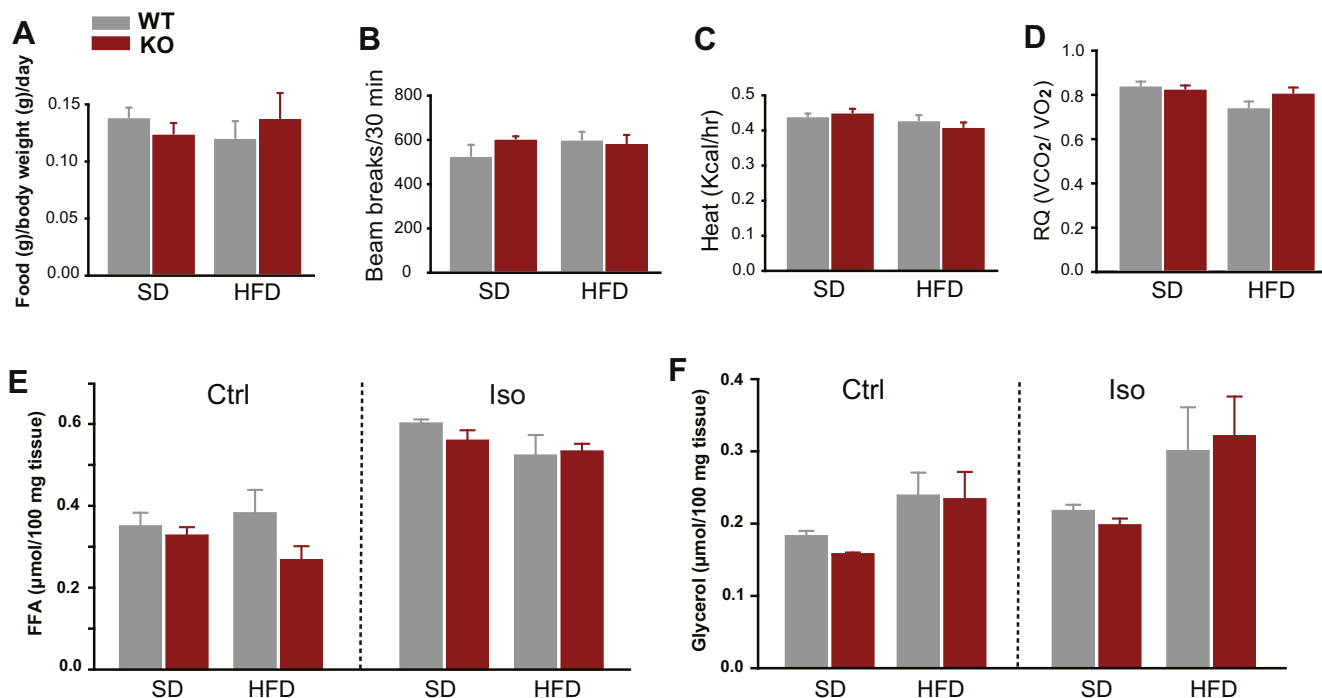


**Fig. 2.** GRK5<sup>-/-</sup> mice did not show significant change in metabolic rates and lipolysis. (A–D) Metabolic parameters determined in a metabolic cage in a 24 h period. Food intake (A), physical activity (B), heat (C), and respiratory quotient (RQ) (D) were measured for 20-week-old WT and GRK5<sup>-/-</sup> mice fed with a SD or HFD.  $n = 6-8$  for each group. (E–F) Basal (Ctrl) and 100 nM isoproterenol (Iso)-stimulated lipolysis, measured by fatty acids (E) and glycerol (F) released from explants of epididymal WAT of 20-week-old WT and GRK5<sup>-/-</sup> mice fed on SD and HFD.  $n = 5-6$  for each group.

intake, locomotor activity, energy production, and respiratory quotient ( $RQ = V_{CO_2}/V_{O_2}$ ) of SD- and HFD-fed mice were determined in metabolic cages over a 24 h period. Despite the differences in body weights,  $GRK5^{-/-}$  mice showed comparable food intake to WT mice no matter on SD or HFD condition (Fig. 2A). Compared with WT mice,  $GRK5^{-/-}$  mice exhibited similar levels of locomotor activity (Fig. 2B) and the basal metabolic rate (Fig. 2C). As shown in Fig. 2D, WT mice fed with HFD expectedly reduced their respiratory quotient (RQ), a measure of fuel-partitioning patterns, however, this seems to not occur in the  $GRK5^{-/-}$  mice, suggesting that  $GRK5$  deficiency might affect the preferential metabolism of fatty acid.

Lipolysis for the liberation of fatty acids that can then be used as an energy source by other tissues is unique to adipocytes. To investigate whether the decreased adiposity observed in  $GRK5^{-/-}$  mice is a result of increased lipolysis, the basal and stimulated glycerol and fatty acid release from WAT explants of WT or  $GRK5^{-/-}$  mice was examined. The rates of glycerol and fatty acid release in adipose tissue of  $GRK5^{-/-}$  mice fed on SD or HFD were not significantly different from those of WT mice under the basal condition or when treated with isoproterenol, which stimulates lipolysis by increasing cAMP levels (Fig. 2E and F).

### 3.3. $GRK5$ deficiency impaired fatty acid synthesis, uptake and oxidation in WAT

As important differences in weight of WAT were observed, we analyzed size of adipocyte from epididymal WAT of  $GRK5^{-/-}$  and WT mice fed a SD or HFD. As shown in Fig. 3A and B, adipocytes from  $GRK5^{-/-}$  mice were smaller than those of wild type. We also examined related mRNA level for enzymes associated with lipid metabolism in epididymal WAT. The expression of genes for both fatty acid synthesis (such as *Agpat2*, *Mgat2*, and *FAS*), fatty acid uptake (such as *Pgc-1b*), and fatty acid oxidation (such as *Mcad*, *Lcad*, and *Cpt-1a*) were significantly down regulated in  $GRK5^{-/-}$  mice feeding with a HFD (Fig. 3C). Taken together, these data suggest that  $GRK5$  is critically involved in the regulation of lipid homeostasis in WAT.

### 3.4. $GRK5$ deficiency reduced adipogenesis

Ablation of  $GRK5$  also resulted in significant down regulation of the expression of adipogenic genes such as PPAR- $\gamma$ , PPAR- $\gamma$  induced genes adiponectin and aP2, C/EBP $\alpha$ , C/EBP $\beta$ , and C/EBP $\delta$  in epididymal WAT from  $GRK5^{-/-}$  mice (Fig. 4A). To gain insight into

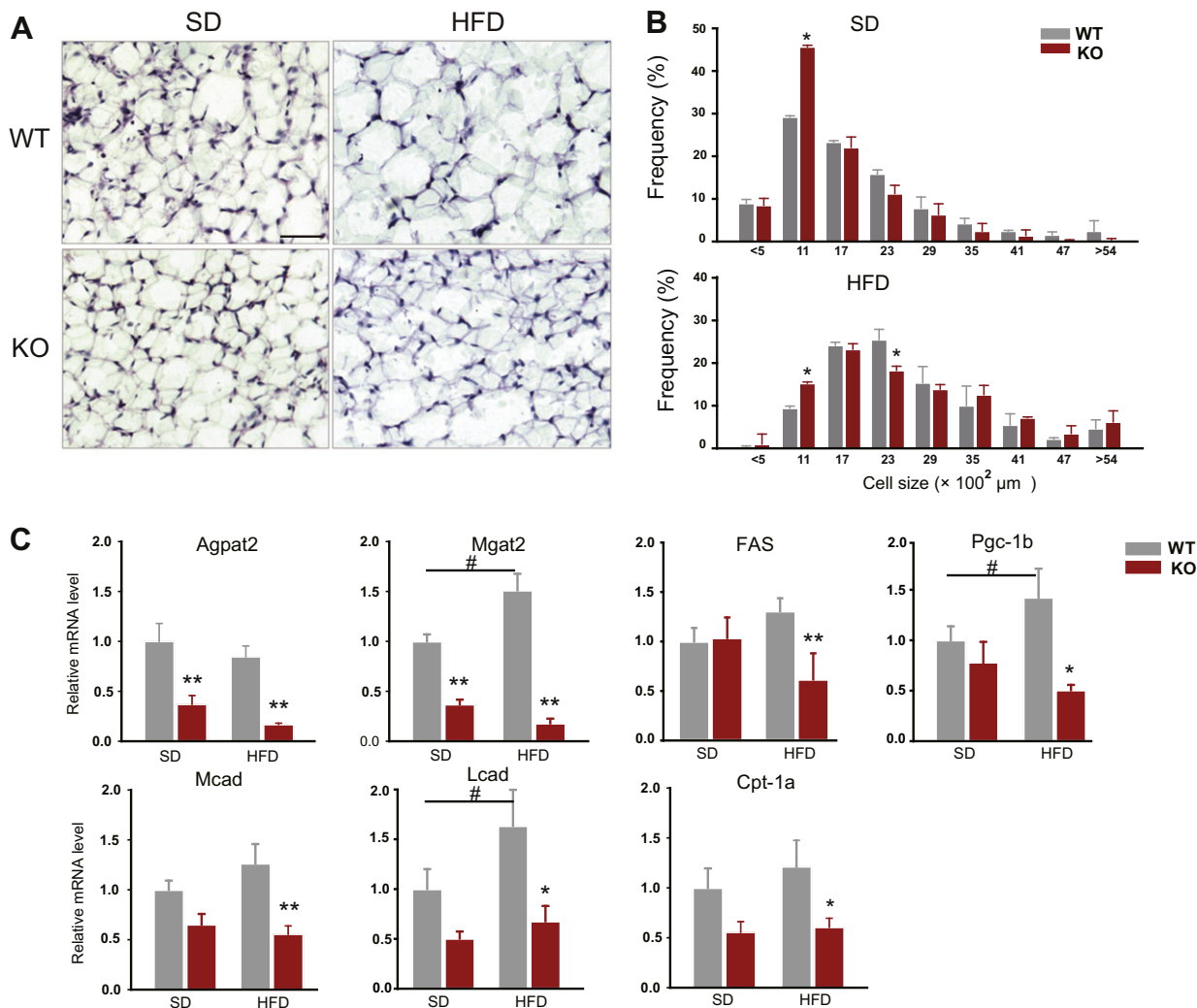


**Fig. 3.**  $GRK5$  ablation impaired fatty acid metabolism in WAT. (A) Representative pictures of H&E-stained paraffin-embedded sections of epididymal WAT from 20-week-old  $GRK5^{-/-}$  and WT mice fed a SD or HFD. Scale bar, 100  $\mu m$ . (B) Distribution of adipocyte size. \* $P < 0.05$  vs. WT group. (C) Quantitative RT-PCR analysis of the expression of WAT genes involved in the fatty acid metabolism of 20-week-old WT and  $GRK5^{-/-}$  mice fed on a SD or HFD.  $n = 6-8$  for each group. \* $P < 0.05$ , \*\* $P < 0.01$  vs. WT group, # $P < 0.05$  vs. SD group.



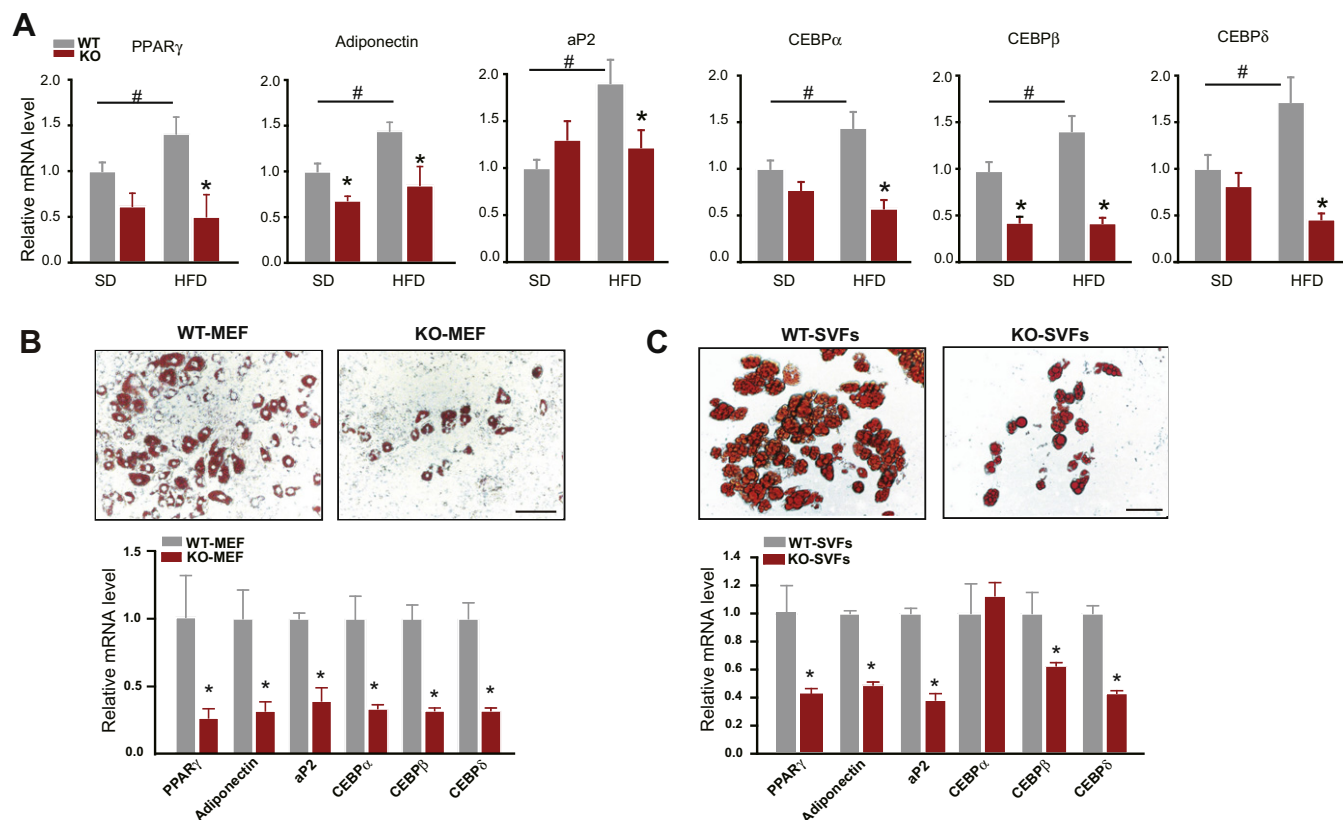


**Fig. 4.** GRK5 ablation impaired adipogenesis in WAT and adipocyte differentiation. (A) Quantitative RT-PCR analysis for the expression of adipocyte differentiation marker genes in epididymal WAT of 20-week-old WT and GRK5<sup>-/-</sup> mice fed a SD and HFD ( $n = 6-8$ ). \* $P < 0.05$  vs. WT group, # $P < 0.05$  vs. SD group. (B and C) MEFs (B) isolated from WT and GRK5<sup>-/-</sup> mouse embryos and SVFs (C) from adult WT and GRK5<sup>-/-</sup> epididymal WAT were differentiated and harvested at day 12. Cells were stained with Oil Red-O (top, scale bar: 100  $\mu$ m) or analyzed by quantitative RT-PCR for the expression of adipocyte differentiation marker genes (bottom, \* $P < 0.05$  vs. WT group). Experiments were performed with cells from 3–5 different embryos or mice.

cellular mechanisms involved in the reduced adiposity, we analyzed adipocyte differentiation in GRK5<sup>-/-</sup> cell lines. MEFs isolated from GRK5<sup>-/-</sup> and WT embryos were induced to differentiate. As shown in Fig. 4B, after differentiation induction, the expression of adipogenic genes such as PPAR- $\gamma$ , adiponectin, aP2, C/EBP $\alpha$ , C/EBP $\beta$ , and C/EBP $\gamma$  was diminished by 50–70% in GRK5<sup>-/-</sup> MEFs compared with WT MEF cells, and GRK5<sup>-/-</sup> cells contained less lipid droplets, a marker of adipocyte differentiation. The recruitment of new adipocytes from precursor cells takes place all lifelong. To determine whether GRK5 is also involved in adipocyte differentiation in adult tissues, SVFs of WAT were isolated from adult GRK5<sup>-/-</sup> and WT mice and these cells were induced to differentiate into adipocytes. As shown in Fig. 4C, Oil Red O-staining indicated a strong reduction of GRK5<sup>-/-</sup> adipocyte formation. Moreover, the expression of PPAR- $\gamma$ , adiponectin, aP2, C/EBP $\beta$ , and C/EBP $\gamma$ , but not C/EBP $\alpha$  was reduced in GRK5<sup>-/-</sup> cells. These results suggest that GRK5 might differentially regulate PPAR $\gamma$ - and C/EBP $\alpha$ -dependent adipogenesis process, from embryonic stages through adulthood.

#### 4. Discussion

The emergence of GRK gene deletion mouse models have helped to reveal the physiological functions of GRKs in vivo. GRK5<sup>-/-</sup> mice were lean at HFD condition. It could not be attributed to potential alterations in food consumption, energy expenditure. However, GRK5 deficiency led to a decrease in level of lipid metabolism and adipogenic gene transcripts in WAT, MEFs, and preadipocytes derived from SVFs of GRK5<sup>-/-</sup> mice. These results

suggest that GRK5 plays a role in the regulation of adipogenesis and is an important endogenous regulator of fat accumulation.

GRKs are known as important kinases that phosphorylate the activated GPCRs to negative regulate GPCR signal transduction. Previous data has demonstrated that elimination of GRK5 results in cholinergic supersensitivity and impaired muscarinic receptor desensitization in brain and lung [16]. It was also shown that under basal, unchallenged conditions, only a slight decrease in body temperature was detected in these mice [16]. This weak phenotype should not contribute to the energy expenditure of GRK5<sup>-/-</sup> mice (Fig. 2A–D). In comparison with GRK5, reduced GRK2 levels also induce a lean phenotype and decrease age-related adiposity [10]. Recent study suggested that increased GRK2 inhibits insulin-stimulated glucose uptake and signaling by a kinase activity-independent mechanism involving the formation of dynamic GRK2/IRS1 complex. The GLUT4 glucose transporter is a key regulator of whole-body glucose homeostasis. Previous study has demonstrated that endogenous GRK2 functions as a negative regulator of insulin-stimulated glucose transport by interfering with G $\alpha$ q/11 signaling to GLUT4 translocation in 3T3-L1 adipocytes [9]. However, regulation of GLUT4 translocation by GRK5 was not observed [9], suggesting that GRK5 may regulate obesity via an alternative pathway.

In this study, we provide evidence that GRK5 positively regulates the adipogenic program and promotes the ability of adipocytes to store lipid. GRK5 deficiency led to a decreased expression of genes related to fat metabolism in WAT (Fig. 3C), and also caused a decrease in the expression of adipose transcription factors genes in vivo and in vitro (Fig. 4). GRK5<sup>-/-</sup> mice showed a large decrease in WAT (Fig. 1C and D), and the GRK5<sup>-/-</sup> MEFs

exhibited the reduced expression of PPAR $\gamma$  and C/EBP $\alpha$  (Fig. 4B). However, GRK5 is not critical for the expression of C/EBP $\alpha$  in SVFs (Fig. 4C). Analysis of the time course of 3T3-L1 differentiation revealed that GRK5 mRNA level rose during differentiation, and GRK5-overexpressing 3T3-L1 cells showed increased expression of PPAR- $\gamma$ , adiponectin, aP2, C/EBP $\beta$ , and C/EBP $\gamma$ , while expression of C/EBP $\alpha$  was not significantly changed (data not shown). These data suggest that GRK5 may promote the differentiation of embryonic fibroblasts and preadipocytes into mature adipocytes via differential regulation of the PPAR $\gamma$ - and C/EBP $\alpha$  expression. Or it might possible that it is the lipogenic process which is mainly affected in adult GRK5 $^{-/-}$  mice.

Future studies will define the role of GRK5 in the metabolic consequences such as insulin resistance, hepatic steatosis, and inflammation of obesity. Furthermore, it remains to be established whether inhibition of catalytic activity, protein expression, or targeted disruption of the specific interaction of GRK5 with differential signaling pathway components are the more appropriate strategies for specifically improving obesity. Additionally, the underlying molecular mechanism remains to be further explored by tissue specific knockout mice.

## Acknowledgments

We thank Dr. W.-P. Jia (Department of Endocrinology and Metabolism, Shanghai Jiaotong University Affiliated Sixth People's Hospital, Shanghai, China) for comments. This research was supported by Grants from the Ministry of Science and Technology (2009CB522006 to L.M.) and the Natural Science Foundation of China (30830042 & 31121061 to L.M., and 30900438 to F.W.).

## References

- [1] G.I. Shulman, Cellular mechanisms of insulin resistance, *J. Clin. Invest.* 106 (2000) 171–176.
- [2] H. Tilg, A.M. Diehl, Cytokines in alcoholic and nonalcoholic steatohepatitis, *N. Engl. J. Med.* 343 (2000) 1467–1476.
- [3] K.L. Spalding, E. Arner, P.O. Westermark, S. Bernard, B.A. Buchholz, O. Bergmann, L. Blomqvist, J. Hoffstedt, E. Naslund, T. Britton, H. Concha, M. Hassan, M. Ryden, J. Frisen, P. Arner, Dynamics of fat cell turnover in humans, *Nature* 453 (2008) 783–787.
- [4] R. Drolet, C. Richard, A.D. Sniderman, J. Mailloux, M. Fortier, C. Huot, C. Rheaume, A. Tchernof, Hypertrophy and hyperplasia of abdominal adipose tissues in women, *Int. J. Obes. (Lond)* 32 (2008) 283–291.
- [5] T.A. Kohout, R.J. Lefkowitz, Regulation of G protein-coupled receptor kinases and arrestins during receptor desensitization, *Mol. Pharmacol.* 63 (2003) 9–18.
- [6] R.J. Lefkowitz, Seven transmembrane receptors: something old, something new, *Acta Physiol. (Oxf)* 190 (2007) 9–19.
- [7] T. Metaye, H. Gibelin, R. Perdrisot, J.L. Kraimps, Pathophysiological roles of G-protein-coupled receptor kinases, *Cell Signal.* 17 (2005) 917–928.
- [8] R.T. Premont, R.R. Gainetdinov, Physiological roles of G protein-coupled receptor kinases and arrestins, *Ann. Rev. Physiol.* 69 (2007) 511–534.
- [9] I. Usui, T. Imamura, H. Satoh, J. Huang, J.L. Babendure, C.J. Hupfeld, J.M. Olefsky, GRK2 is an endogenous protein inhibitor of the insulin signaling pathway for glucose transport stimulation, *Embo J.* 23 (2004) 2821–2829.
- [10] L. Garcia-Guerra, I. Nieto-Vazquez, R. Vila-Bedmar, M. Jurado-Pueyo, G. Zalba, J. Diez, C. Murga, S. Fernandez-Veledo, F. Mayor Jr., M. Lorenzo, G protein-coupled receptor kinase 2 plays a relevant role in insulin resistance and obesity, *Diabetes* 59 (2010) 2407–2417.
- [11] X. Jiang, P. Yang, L. Ma, Kinase activity-independent regulation of cyclin pathway by GRK2 is essential for zebrafish early development, *Proc. Natl. Acad. Sci. USA* 106 (2009) 10183–10188.
- [12] J.S. Martini, P. Raake, L.E. Vinge, B.R. DeGeorge Jr., J.K. Chuprun, D.M. Harris, E. Gao, A.D. Eckhart, J.A. Pitcher, W.J. Koch, Uncovering G protein-coupled receptor kinase-5 as a histone deacetylase kinase in the nucleus of cardiomyocytes, *Proc. Natl. Acad. Sci. USA* 105 (2008) 12457–12462.
- [13] D. Sorriento, M. Ciccarelli, G. Santulli, A. Campanile, G.G. Altobelli, V. Cimini, G. Galasso, D. Astone, F. Piscione, L. Pastore, B. Trimarco, G. Iaccarino, The G-protein-coupled receptor kinase 5 inhibits NF $\kappa$ B transcriptional activity by inducing nuclear accumulation of IkappaB alpha, *Proc. Natl. Acad. Sci. USA* 105 (2008) 17818–17823.
- [14] X. Chen, H. Zhu, M. Yuan, J. Fu, Y. Zhou, L. Ma, G-protein-coupled receptor kinase 5 phosphorylates p53 and inhibits DNA damage-induced apoptosis, *J. Biol. Chem.* 285 (2010) 12823–12830.
- [15] T.J. Bartness, C.K. Song, Thematic review series: adipocyte biology. Sympathetic and sensory innervation of white adipose tissue, *J. Lipid Res.* 48 (2007) 1655–1672.
- [16] R.R. Gainetdinov, L.M. Bohn, J.K. Walker, S.A. Laporte, A.D. Macrae, M.G. Caron, R.J. Lefkowitz, R.T. Premont, Muscarinic supersensitivity and impaired receptor desensitization in G protein-coupled receptor kinase 5-deficient mice, *Neuron* 24 (1999) 1029–1036.